Non-Concerted Cope Rearrangement

Wolfgang R. Roth†*[a], Rolf Gleiter*[b], Volker Paschmann[a], Ulrich E. Hackler[a], Gerd Fritzsche[b], and Holger Lange[b]

Fakultät für Chemie der Universität Bochum[a],
Postfach 10 21 48, D-44780 Bochum, Germany

Organisch-Chemisches Institut der Universität Heidelberg[b],
Im Neuenheimer Feld 270, D-69120 Heidelberg, Germany

Received September 8, 1997

Keywords: Diradicals / Dioxygen trapping / Diradical well / Heat of formation / Ab initio calculations

The observation of practically identical activation parameters for the Cope rearrangement **2**→**6** and its "frustrated" counterpart **1**→**5** indicates a two-step mechanism for the reaction **2**→**6**. Direct proof of this interpretation comes from trapping experiments, which demonstrate the intermediate formation of the diradicals **5** and **9**. From the temperature and oxygen dependences of the trapping rates, recombination barriers of $\Delta H^{\neq}$ = 11.5 and 6.5 kcal·mol^{-1} have been derived for **5**→**1** and **9**→**6**, respectively. These results agree well with ab initio calculations (CASPT2).

Recently, the syntheses, properties and reactions of the highly strained polyenes **1**–**4** have been reported.[1] For the Cope rearrangement leading to **6**–**8**, a two-step mechanism must be considered in view of the highly strained nature of starting materials and the products, respectively. In 1,5-hexadiene, the non-concerted pathway is destabilized by 59.7[2]–33.5[3] = 26.2 kcal·mol^{-1}; this could not be counterbalanced by the introduction of radical stabilizing substituents[4] because a comparable stabilization was also observed for the concerted route.

Scheme 1. Cope-rearrangement of 1,5-hexadiene systems

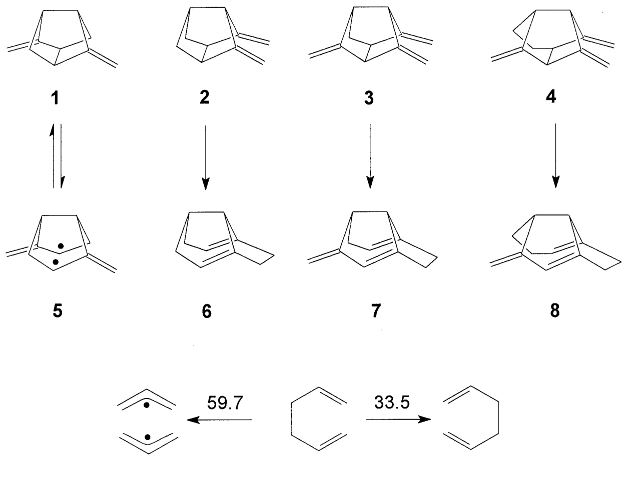

A completely different situation must be envisaged in the case of **2**, **3**, and **4**. Here, the concerted route should be rendered more difficult because of the steric hindrance that occurs when the terminal carbon atoms of the 1,5-hexadiene moiety approach each other. X-ray investigations on stelladiene derivatives have shown that the distance between the termini of the exomethylene groups amounts to 4.12–4.20 Å and that the central bonds are elongated to 1.61–1.62 Å.[5] In this paper, we report on our attempts to establish the two-step nature of the rearrangement **2**→**6** through oxygen-trapping experiments. In a concluding section, the experimental results are compared with ab initio calculations for the systems in question.

1. Equilibrium 1 ⇄ 5

The "frustrated" Cope rearrangement **1** ⇄ **5** should be an adequate reference system for the two-step Cope rearrangement **2**→**6** and should be amenable to kinetic analysis by trapping of the diradical **5**.

Indeed, gas-phase thermolysis of **1** in the presence of dioxygen leads to a decrease in the substrate concentration, which follows strictly pseudo-first-order kinetics; no formation of new products of low molecular weight could be observed. The rate of the reaction was measured at five temperatures (90–130°C), each at four different oxygen pressures (0–1000 mbar). The resulting rates are listed in Table 4 and their oxygen dependence is shown graphically in Figure 1.

Figure 1. Oxygen dependence of the trapping rate of **5**

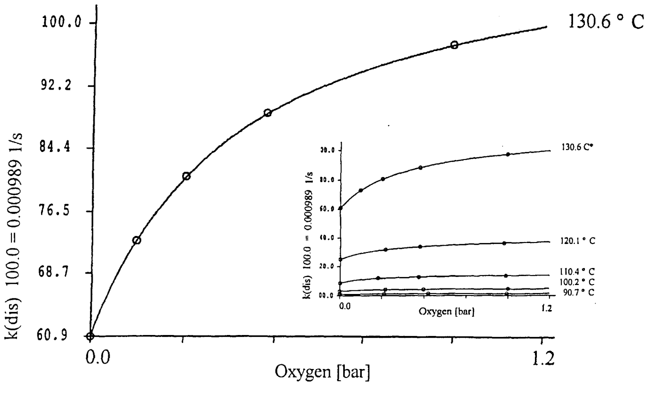

The curvature of the graph meets with expectation for the trapping of an intermediate in a preequilibrium (Scheme 2).

At low oxygen pressures, the rate decrease shows a linear dependence on the oxygen concentration, because the equilibrium **1** $\rightleftharpoons$ **5** is still established here. At high concentrations of the trapping agent, under which conditions all intermediate diradicals are trapped, the rate decrease asymptotically approaches a limiting value, corresponding to the rate constant $k_{1,5}$. To calculate $k_{5,1}$, knowledge of k_s, the rate constant that describes the reaction of **5** with oxygen, is essential. It has been shown repeatedly[6] that radicals as well as diradicals react with oxygen in a collision-controlled fashion,[7] so that this assumption seems to be justified here as well. Though the absolute value of the rate constant k_s is thus not known with high accuracy, it does not affect the calculated activation enthalpy. Since k_s represents a collision-controlled reaction, its temperature dependence follows a $T^{1/2}$ law, and only this relation enters the calculation of the activation enthalpy. The uncertainty in k_s on the other hand appears only in the A-factor of the reaction.

Scheme 2. Mechanism for the trapping of **5**

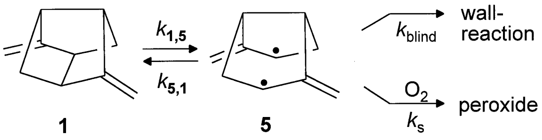

$$k_{dis} = k_{1,5} \bullet \left(1 - \frac{k_{5,1}}{k_{5,1} + k_{blind} + k_s \bullet [O_2]} \right) s^{-1} \qquad (1)$$

The analysis is somewhat affected by the high background rate of the thermolysis reaction. Even in the absence of oxygen, one observes a significant decrease in the substrate concentration, which strictly obeys pseudo-first-order kinetics. Noteworthy is the fact that the activation energy for this reaction resembles that for the formation of the diradical **5** (E_a = 28.9 kcal·mol^{-1}; log A = 12.4). Obviously, **5** can also be trapped through reaction with the wall of the flask, a reaction that has been observed with other long-living diradicals.[8] In Figure 1, the intercept corresponds to the contribution from this reaction.

Evaluation of the data in Table 4 (Experimental Section) has been performed by simulation of the reactions shown in Scheme 2 using a simplex routine.[9] The resulting activation parameters are summarized in Table 1. Starting with a force-field value[10] for the heat of formation of **1**, the aforementioned activation enthalpies allow the construction of the energy profile for the trapping reaction of **5**, as depicted in Figure 2. The resulting heat of formation for the intermediate diradical **5** is in satisfactory agreement with the calculated force-field[10] value for this species (81.2 vs. 80.0 kcal·mol^{-1}). Using the reaction force-field MMEVBH,[10] one obtains for the transition state of the reaction a heat of formation that comes close to the experimental value (94.4 vs. 92.5 kcal·mol^{-1}).

2. Rearrangement 2→6

In the gas phase at temperatures >100°C, **2** quantitatively forms the diene **6**[12]. From the first-order rate constants (Table 5), determined at five different temperatures (90−130°C), one can derive the activation parameters listed in Table 1.

In the presence of oxygen, the gas-phase thermolysis of **2** shows in addition to the formation of **6**, an overall loss of mass. In analogy to the thermolysis of **1**, no new low molecular weight products could be detected. The reaction was monitored at five temperatures (90−130°C), each at up to four different oxygen pressures. The resulting first-order rate constants for the trapping and consumption of the substrate are summarized in Table 5 (Experimental Section).

As can be seen from the data in Table 5, the rate of decrease in the starting material concentration exhibits a linear dependence on the oxygen pressure at high oxygen concentrations. This indicates a bimolecular reaction of the substrate with oxygen, in analogy to the behavior of other molecules with highly strained σ-bonds, e.g. 1,3,5-[2.2.2]paracyclophane[8] or octamethylsemibullvalene.[13]

At low temperatures, at which the rearrangement **2**→**6** is negligible, the bimolecular reaction can be observed independently. Using the rate constants in Table 5 (Experimental Section), the activation parameters shown in Table 1 were derived.

However, the observed overall loss of mass during the thermolysis of **2** in the presence of oxygen is significantly larger than the mass loss attributable to the bimolecular reaction alone. Because the rearrangement product **6** does not react with oxygen, this indicates a partial trapping of the diradical **9**. If one accepts that, in analogy with the trapping experiments of **5**, the reaction of **9** with oxygen is also collision-controlled, the ratio of trapping and rearrangement products allows calculation of the rate constant $k_{9,6}$, which leads to the activation parameters shown in Table 1.

The oxygen pressure dependence of the observed reaction is in accord with an interpretation based on the trapping of an intermediate species. As can be seen in Figure 2, this dependence varies asymptotically from a nonlinear to a linear behavior at high oxygen pressures. The linear part describes the situation where all intermediate diradicals are trapped quantitatively, i.e. here the slope of the graph is caused by the bimolecular reaction of the substrate with oxygen. At low temperatures, where the formation of **9** can be ignored, the graph shows only the linear dependence over the whole pressure range, in agreement with the bimolecular reaction now being the sole reaction.

The observation that at high oxygen concentrations the rate of consumption of **2**, after correction for the bimolecular reaction, exhibits no further dependence on the oxygen pressure, underlines that there is no reverse reaction **9**→**2** to speak of. This means that the energy difference between the transition states leading to **9** and **6** must be >3−4 kcal·mol^{-1}. However, the trapping experiments do not al-

Figure 2. Enthalpy diagram [kcal · mol^{-1}] for the trapping of **5** and **9**. The calculated (cal.) values are based on the ab initio calculation. The values given for the heat of formation of **1**, **2** and **6** are derived from force field calculations.[10]

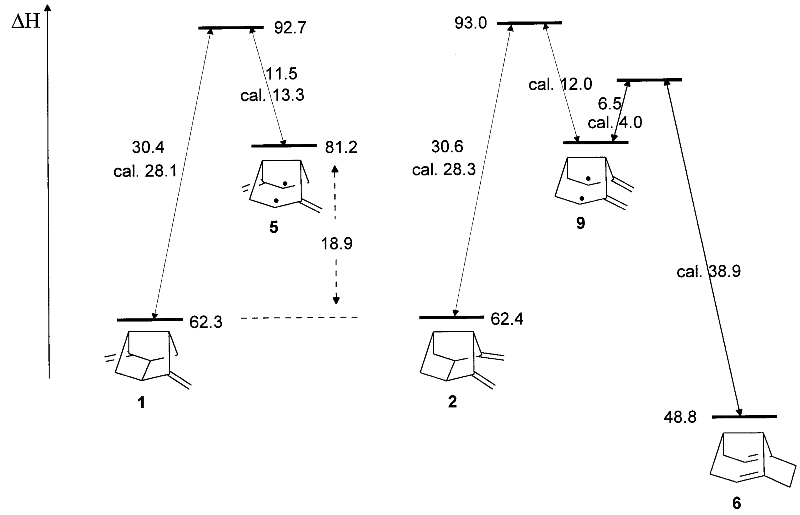

Table 1. Activation parameters[a]

Reaction	T_m[b]	E_a[c]	log A	$\Delta H^{\neq}$[c]	$\Delta S^{\neq}$[d]
$k_{1,5}$	110	31.2±0.4	13.97±0.24	30.4±0.4	3.09±1.14
$k_{5,1}$	110	12.3±0.5	14.75±0.31	11.5±0.5	6.67±1.41
$k_{2,6}$	110	31.4±0.2	13.94±0.24	30.6±0.2	2.74±0.48
k_{bi}	113	19.6±0.5	8.53±0.26	18.8±0.5	−20.99±1.17
$k_{9,6}$	116	7.3±0.6	12.33±0.16	6.5±0.6	−4.62±1.11

[a] Uncertainty limits are based on a 95% confidence level and have been calculated for data obtained by simulation by the method of Nelder.[11] – [b] [°C]. – [c] [kcal · mol^{-1}]. – [d] [cal · K^{-1} · mol^{-1}].

Scheme 3. Reaction of strained 1,5-hexadiene systems with oxygen

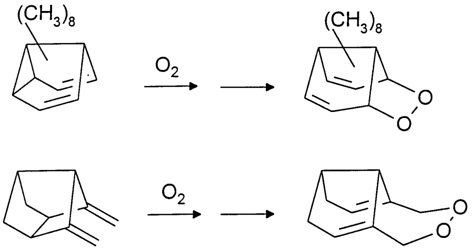

Scheme 4. Mechanism for the thermolysis of **2** in the presence of oxygen

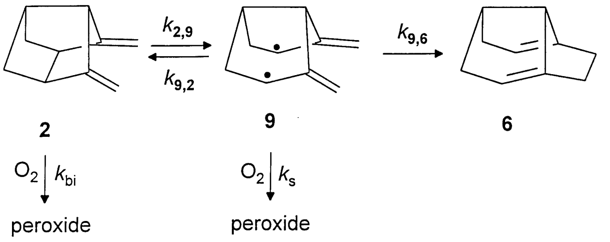

low a precise determination of this difference. If, in accordance with force-field calculations,[10] one assumes that the heats of formation of **5** and **9** are comparable, then one obtains the energy profile for the Cope rearrangement **2**→**6** shown in Figure 2. In line with a two-step mechanism, practically identical activation enthalpies are found for the reactions of **1** and **2**. The bond-breaking step of the Cope rearrangement **2**→**6** is not supported by the concerted formation of the new [3,3] bond.

Figure 3. Oxygen dependence of the loss of mass in the thermolysis of **2**

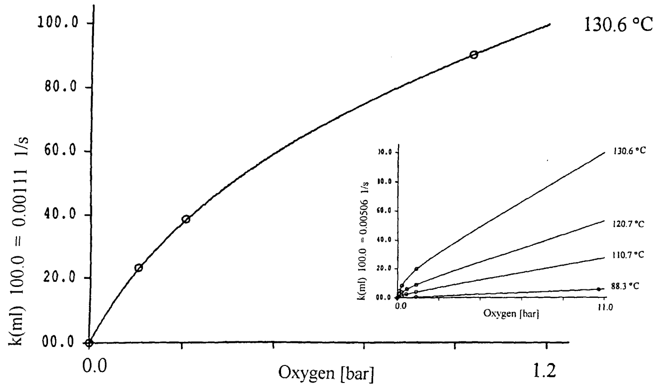

Scheme 5. Mechanism for the reaction of **2** with oxygen

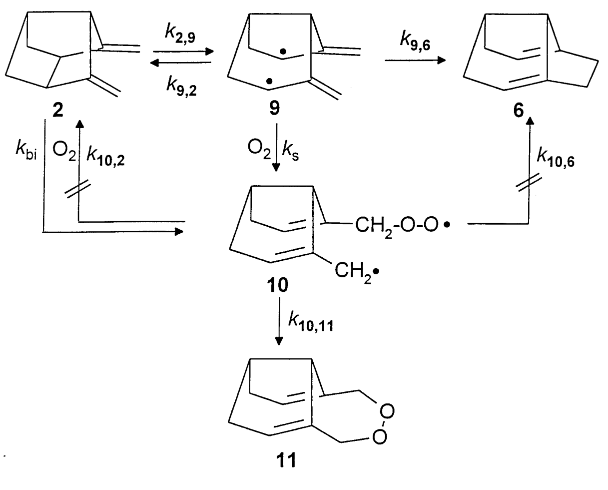

The peroxy diradical **10**, i.e. the primary product of both the trapping of **9** and the bimolecular reaction of the substrate with oxygen, should be able to decompose either to the product **6** or, as a reversal of its formation, to the starting material **2**. With a reaction enthalpy $\Delta H_R(\mathbf{2},\mathbf{9}) = 17.6$ kcal·mol^{-1} (Scheme 2), the energy of the C−OO$^{\bullet}$ bond of 31.5 kcal·mol^{-1}[14] and an allyl stabilization energy of 13.5 kcal·mol^{-1}[10], the reaction with the starting material should be practically thermoneutral [$\Delta H_R(\mathbf{2},\mathbf{10}) = -17.6 + 31.5 - 13.5 = 0.4$ kcal·mol^{-1}]. The formation of **6**, on the other hand, should be correspondingly exothermic. However, trapping experiments in supercritical carbon dioxide with an oxygen pressure of 11 bar[15] show that the decay **10**→**6** does not occur. Otherwise, at low temperatures, at which the rearrangement **2**→**6** is negligible, formation of **6** should have been observed, which was not the case. This clearly indicates that the intramolecular cyclization **10**→**11** is the dominant reaction channel for the stabilization of **10**. Furthermore, it also explains why in the case of **1**, where the equivalent cyclization is not possible, no bimolecular reaction of the substrate with oxygen could be observed.

3. Discussion

The Cope rearrangement demonstrates impressively how the mechanism of a reaction can be manipulated through the introduction of substituents.

For the parent system, a concerted mechanism[16] with a distinct preference for the chair over the boat geometry of the transition state has been demonstrated.[17] Its heat of formation ($\Delta H_f^0 = 53.6$ kcal·mol^{-1})[3] lies 9.0 kcal·mol^{-1} below that of 1,4-cyclohexanediyl ($\Delta H_f^0 = 62.6$ kcal·mol^{-1})[18].

If one or both double bonds of the 1,5-hexadiene moiety become part of a cumulated system, the two-step reaction path is able to compete with the concerted mechanism. In the thermolysis of 1,2,6-heptatriene, the 2-methylene-1,4-cyclohexanediyl is a trappable species[18], its heat of formation ($\Delta H_f^0 = 69.4$ kcal·mol^{-1})[18] lying 10.6 kcal·mol^{-1} below that for the concerted transition state ($\Delta H_f^0 = 80.0$ kcal·mol^{-1})[18].

Scheme 6. Mechanism for the Cope-rearrangement [kcal · mol-1]

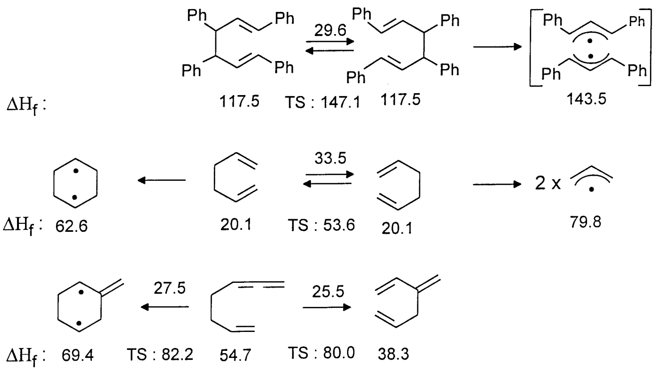

Attempts to assist the decay of 1,5-hexadiene into two allyl radicals through conjugative stabilization, so that this pathway lies below the concerted one in energy, have led to the formation of radical pairs. Despite the fact that their heat of formation is smaller than the heat of formation of the transition state of the concerted reaction, a decay into free allyl radicals does not occur.[19]

The Cope rearrangement of **2** adds a new variant to the aforementioned mechanistic range. The decay of the 1,5-hexadiene moiety into two allyl radicals is supported here by the release of strain energy, i.e. the two-step mechanism becomes the energetically favoured one.

The rate-determining step in the thermolysis of **2** is the formation of the intermediate diradical **9**. Even though an interaction between the ends of the 1,5-hexadiene moiety is possible, the transition state of the reaction is not affected by this possibility. This leads to practically identical activation parameters for the bond-breaking step in **1** and **2**, respectively. To assist the breaking of the central carbon-carbon bond in **2**, i.e. to support the concerted pathway, the terminal olefinic carbons would have to approach each other by approximately 3 Å. According to force-field[10] calculations this would require an energy of 15.6 kcal·mol^{-1}, which is too large to be compensated for by the energy gained in the concerted reaction. The two-step mechanism is thus, as demonstrated by the trapping of **9**, the energetically favoured alternative.

A comparison of the reaction of **2** with the analogous rearrangement of semibullvalene **12** is informative. The reaction enthalpies for the formation of the corresponding bis(allyl) radicals are, according to force-field[10] calculations, of comparable magnitude (17.1 vs. 16.0 kcal·mol^{-1}). However, the activation energies for these Cope rearrangements differ from each other by 31.2 − 5.4[20] = 25.8 kcal·mol^{-1}. As a first approximation, this corresponds to the steric energy ($E_{st} = 27$ kcal·mol^{-1}), that is required to reduce the distance between the terminal carbons of the 1,5-hexadiene moiety, so that this distance resembles that of the corresponding carbon atoms in the semibullvalene framework, i.e. 2.4 Å.

Scheme 7. Comparison of the concerted and non-concerted Cope-rearrangement of **2** and **12** [kcal · mol-1]

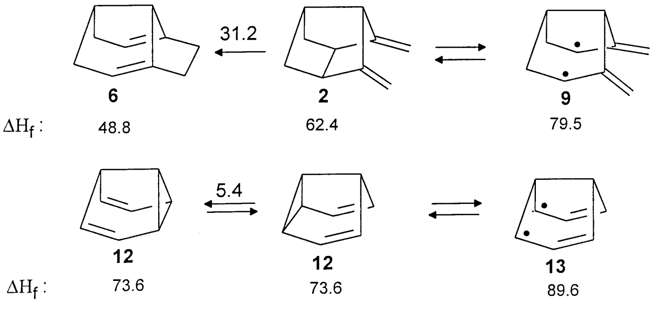

In contrast to **2**, the diradical **13** cannot be trapped with oxygen because here the bimolecular reaction of **12** with oxygen becomes the dominant process.[21]

4. Quantum Chemical Calculations

The Cope rearrangement has been repeatedly investigated by quantum chemical methods[22][23]. In the course of our studies, the geometries of the closed-shell systems **1**, **2**, and **6** were calculated using the restricted Hartree-Fock (RHF) method, whereas the open-shell systems (**5**, **9**) and the transition states (TS-**1**,**5**, TS-**2**,**9**, TS-**2**,**6**, TS-**9**,**6**) were calculated using the CASSCF method[24]. The latter allows a correct description of open-shell electronic states. The relative energies of these systems were then determined by the CASPT2 procedure[25], which introduces a second-order pertubational correction to the CASSCF wavefunction. In this way, the effects of degeneracy correlation (CASSCF) as well as those of the dynamic correlation (CASPT2) are taken into account. To derive the thermodynamic data of interest, the stationary points on the energy surface were subjected to a frequency analysis. The CASPT2 energies were then corrected accordingly.

The starting materials **1** (D_2) and **2** (C_S), the product **6** (C_S), as well as the concerted transition state TS-**2**,**6** (C_S) were geometry optimized at the RHF level, whereas the diradicals **5** (C_2) and **9** (C_S)[26] as well as the transition states TS-**1**,**5** (C_2), TS-**2**,**9** (C_S), and TS-**9**,**6** (C_S) were optimized at the CASSCF level of theory. The latter encloses the active space of six electrons in six orbitals, a so-called CASSCF(6,6). The six orbitals correspond to both π- and π*-MOs and the σ- and σ*-MOs of the breaking bond. At these levels (RHF and CASSCF, respectively) the frequency analyses were carried out. To determine the thermochemical data, the unscaled frequencies were used (T = 298.15 K). The pertubational correction of the CASPT2 energies was based on the CASSCF(6,6) wavefunction in the case of the diradicals and transition states, respectively. For starting materials and products, an active space was chosen that included both π- and π*-MOs [CASSCF(4,4), four electrons in four MOs]. One can demonstrate that the absolute CASPT2 energies change only very little if one expands the active space from (4,4) to (6,6) ($\Delta E < 2$ kcal·mol^{-1}). For all calculations, the 6-31G* basis set[27] was used, a valence double-ζ-basis with polarization functions at the carbon atoms. The RHF and CASSCF calculations were performed with the GAUSSIAN-94 program[28]; the CASPT2 calculations with the MOLCAS-3 program[29].

The activation parameters for the equilibrium **1** $\rightleftharpoons$ **5** are summarized in Table 3, while the most important bond lengths in **1**, TS-**1**,**5** and **5** are presented in Figure 4. For the singlet diradical ^{1}**5**, the distance between the carbons of the broken bond is so large (3.842 Å) that a through-space interaction can be ruled out.

Figure 4. Selected bond lengths of **1** (RHF/6-31G*), TS-**1**,**5** [CASSCF(6,6)/6-31G*], and **5** [CASSCF(6,6)/6-31G*] in Å

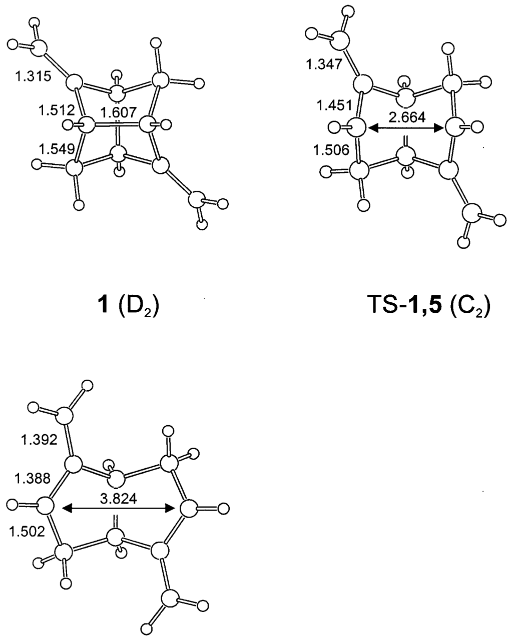

1 (D_2) TS-**1**,**5** (C_2)

^{1}**5** (C_2)

The ground state of the starting material **1** is dominated by a single determinant, which in the CASSCF(4,4) wavefunction accounts for 93% of its weight, while no other determinant accounts for more than 3%. This justifies the closed-shell approach for **1**. In the transition state TS-**1**,**5**, this configuration,

$$\varphi_0 = |\ldots (18a)^2(19a)^2(16b)^2(17b)^2 >$$

has only a weighting of 73%, and is followed by the shell-opening double excitation

$$\varphi_1 = |\ldots (18a)^2(16a)^2(17b)^2(18b)^2 >$$

having a weighting of 16%. In the diradical, the contribution of φ_1 grows to 39%, whereas that of φ_0 decreases to 46%. The ratio of the squares of the coefficients, $c_0{}^2/c_1{}^2$, therefore, amounts to 1.17, which is fairly close to the ideal value of 1.0 for a "perfect" diradical. Table 2 shows the occupancy numbers of the active MOs and the ratios of their coefficients. The singlet/triplet gap amounts to only −0.3 kcal·mol^{-1}. It is noteworthy that the singlet species forms the ground state, a known contradiction of Hund's rule.[30]

Table 2. Occupation numbers of the natural orbitals which are included into the active space and squares of coefficients of the most important determinants of the CASSCF wave function

	1	TS-**1**,**5**	Diradical ^{1}**5**	Diradical ^{3}**5**
18*a*	x	1.91	1.91	1.90
19*a*	1.93	1.61	1.07	1.00
20*a*	0.08	0.09	0.10	0.10
17*b*	1.92	1.91	1.90	1.90
18*b*	0.07	0.40	0.93	1.00
19*b*	x	0.08	0.09	0.10
$c_0{}^2/c_1{}^2$	115	4.56	1.17	48
$c_0{}^2$	0.93	0.73	0.46	0.85

Regarding the Cope rearrangement **2**→**6**, one finds on the RHF level a single-step pathway, whereas on the CASSCF level of theory, a two-step mechanism is found and the concerted pathway vanishes on the potential energy surface. The activation parameters are summarized in Table 3 and selected bond lengths of TS-**2**,**9**, ^{1}**9**, and TS-**2**,**6** are presented in Figure 5. Note that at 2.865 Å the σ-bond length in the concerted TS-**2**,**6** is larger than that in TS-**2**,**9**

(2.681 Å). From a geometrical point of view, this indicates that TS-**2**,**6** is more bis-allylic than aromatic in character. In the case of an aromatic transition state, one would expect an interallylic distance of approximately 2.2 Å on the RHF/6-31G* level.[23]

A comparison of the geometrical parameters of the transition states TS-**2**,**9** and TS-**1**,**5** and of the diradicals ^{1}**5** and ^{1}**9** reveals a great resemblance between them. Also, the first step of the reaction, the bond-breaking of the central σ-bond, is energetically identical for both reactions. This means that the hexacyclic orientation in **2**, typical for the transition state of a Cope rearrangement, leads to no stabilization whatsoever. The singlet/triplet gap of the diradical **9** is again small, amounting to -0.9 kcal/mol^{-1}.

Figure 5. Selected bond lengths of TS-**2**,**9** [CASSCF(6,6)/6-31G*], ^{1}**9** [CASSCF(6,6)/6-31G*], and TS-**2**,**6** (RHF/6-31G*) in Å

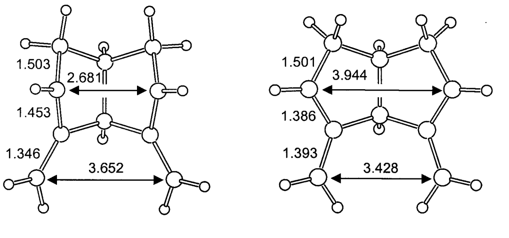

TS-**2**,**9** (C_s) ^{1}**9** (C_s)

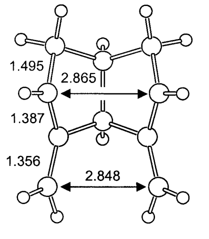

TS-**2**,**6** (C_s)

Table 3. Activation parameters of the calculated reactions

Reaction	$\Delta H^{\neq}$[a]	$\Delta S^{\neq}$[b]
$k_{1,5}$	28.1	4.40
$k_{5,1}$	13.3	−4.99
$k_{2,9}$	28.3	3.26
$k_{9,2}$	12.0	−1.19
$k_{9,6}$	4.0	0.86
$k_{6,9}$	38.9	2.81
$k_{2,6}$	29.5	0.75
$k_{6,2}$	48.1	−1.75

[a] [kcal · mol^{-1}]. – [b] [cal · K^{-1} · mol^{-1}].

The calculated values are in satisfactory agreement with the corresponding experimental values. However, correct energies have been obtained only by the use of second-order perturbation theory (CASPT2). At the present time it is not possible to calculate gradients at this level of theory, which means that the geometries must be optimized on the RHF and CASSCF levels, respectively, a procedure that has proved not to be without its inherent difficulties, as was shown by calculations of the Cope rearrangement of 1,5-hexadiene.[23] We are currently investigating whether such behavior may play some role in the calculations of the systems described in this paper. However, our first results indicate that the two-step mechanism remains the preferred one, even on the CASPT2 level. Whether the concerted pathway is a mechanistic alternative remains to be seen. A substantial difference with respect to the parent system originates from the rigidity of the stellane framework, which limits its flexibility and, consequently, affects the geometrical course of the reaction. In view of this, a fundamental mechanistic change must be ruled out.

Theory and experiment agree on the point that the Cope rearrangement of the stellane framework follows a two-step mechanism with a singlet diradical as intermediate. However, the ab initio calculations indicate that, at least as a side-reaction, the concerted pathway is still a possibility.

The *ortho*-stelladiene **2** therefore constitutes a borderline case, having similar energies for the concerted- and the two-step pathway. As a consequence, we are currently investigating the influence of the enlargement of the bridge that leads to the homologous twistbrendadiene series, as well as the effect of additional double bonds. While the first manipulation should favour the concerted pathway, we expect the latter to facilitate the two-step mechanism.

We are grateful to the *Deutsche Forschungsgemeinschaft* and the *Fonds der Chemischen Industrie* for financial support. H. L. thanks the *Studienstiftung des Deutschen Volkes* for a stipend.

Experimental Section

1. Kinetic Measurements: The rate constants, listed in Tables 4 and 5, were measured using the technique and apparatus described previously.[31]

Table 4. Rate constance for the disappearance of **1** in the presence of oxygen

Temp [°C]	90.70	90.70	90.70	90.70	
O_2 [mbar]	0.0	256.0	506.0	954.0	
k_{dis} · 104 [s^{-1}]	0.1152	0.1486	0.1554	0.1598	
Temp [°C]	100.2	100.2	100.2	100.2	
O_2 [mbar]	0.0	263.0	479.0	962.0	
k_{dis} · 104 [s^{-1}]	0.3156	0.4253	0.4493	0.4699	
Temp [°C]	110.40	110.4	110.4	110.4	
O_2 [mbar]	0.0	219.0	450.0	947.0	
k_{dis} · 103 [s^{-1}]	0.0872	0.1187	1.300	1.394	
Temp [°C]	120.1	120.1	120.1	120.1	
O_2 [mbar]	0.0	260.0	455.0	935.0	
k_{dis} · 103 [s^{-1}]	0.2544	0.3203	0.3431	0.3704	
Temp [°C]	130.6	130.6	130.6	130.6	130.6
O_2 [mbar]	0.0	116.0	244.0	456.0	953.0
k_{dis} · 103 [s^{-1}]	0.6266	0.7325	0.8106	0.8936	0.9927

Table 5. Rate constance for the thermolysis of **2** in the presence of oxygen

Temp [°C]	90.1	92.4	88.4	100.8	100.7	110.8
O_2 [mbar]	0.0	1005.3	10710	0.0	1005.1	0.0
$k_{\mathbf{2,6}} \cdot 103$ [s^{-1}]	0.0109			0.0386		0.1136
$k_{bi} \cdot 102$ [$M^{-1}s^{-1}$]		0.0951	0.0891		0.1912	
$k_{ml} \cdot 103$ [s^{-1}]		0.0392	0.3269		0.0934	
$k_{\mathbf{9,6}} \cdot 109$ [s^{-1}]		0.0898			0.1137	
Temp [°C]	109.8	109.7	111.2	120.7	120.4	120.4
O_2 [mbar]	251.8	503.7	1005.3	0.0	254.7	506.5
$k_{\mathbf{2,6}} \cdot 103$ [s^{-1}]				0.3232		
$k_{bi} \cdot 102$ [$M^{-1}s^{-1}$]	0.3754	0.3754	0.3754		0.7079	0.8089
$k_{ml} \cdot 103$ [s^{-1}]	0.0844	0.1334	0.2082		0.1899	0.2992
$k_{\mathbf{9,6}} \cdot 109$ [s^{-1}]	0.1441	0.1481	0.1401		0.1899	0.1939
Temp [°C]	119.9	130.6	131.7	131.7	131.7	
O_2 [mbar]	999.1	0.0	126.7	249.2	1002.8	
$k_{\mathbf{2,6}} \cdot 103$ [s^{-1}]		0.8610				
$k_{bi} \cdot 102$ [$M^{-1}s^{-1}$]	0.7599		1.294	1.396	1.410	
$k_{ml} \cdot 103$ [s^{-1}]	0.4540		0.2381	0.4031	0.9812	
$k_{\mathbf{9,6}} \cdot 109$ [s^{-1}]	0.1859		0.2298	0.2418	0.2258	

---

[1] R. Gleiter, B. Kissler, *Tetrahedron Lett.* **1985**, *26*, 185−188; **1987**, *28*, 6151−6154; R. Gleiter, B. Kissler, C. Ganter, *Angew. Chem.* **1987**, *99*, 1292−1294; *Angew. Chem. Int. Ed. Engl.* **1987**, *26*, 1252−1253; R. Gleiter, C. Sigwart, B. Kissler, *ibid.* **1989**, *101*, 1561−1563; **1989**, *28*, 1525-1526; R. Gleiter, C. Sigwart, *J. Org. Chem.* **1994**, *59*, 1027−1038; R. Gleiter, T. Herb, O. Borzyk, I. Hyla-Kryspin, *Liebigs Ann.* **1995**, 357−364.

[2] W. R. Roth, F. Bauer, A. Beitat, T. Ebbrecht, M. Wüstefeld, *Chem.Ber.* **1991**, *124*, 1453−1460.

[3] W. v. E. Doering, V. G. Toscano, G. H. Beasley, *Tetrahedron*, **1971**, *27*, 5299−5306.

[4] W. R. Roth, F. Hunold, *Liebigs Ann.* **1996**, 1917−1928.

[5] V. Siemund, H. Irngartinger, C. Sigwart, B. Kissler, R. Gleiter, *Acta Crystallogr.* **1993**, *C49*, 57.

[6] W. R. Roth, T. Bastigkeit, S. Börner, *Liebigs Ann.* **1996**, 1323−1328.

[7] W. R. Roth, T. Schaffers, M. Heiber, *Chem. Ber.* **1992**, *125*, 739−749.

[8] W. R. Roth, H. Hopf, A. de Meijere, F. Hunold, S. Börner, M. Neumann, T. Wasser, J. Szurowski, C. Mlynek, *Liebigs Ann.* **1996**, 2141−2154.

[9] S. N. Demming, S. L. Morgan, *Anal. Chem.* **1973**, *45*, 278A−283A.

[10] W. R. Roth, V. Staemmler, M. Neumann, C. Schmuck, *Liebigs Ann.* **1995**, 1061−1118.

[11] J. A. Nelder, R. Mead, *Comput. J.*, **1965**, *7*, 308−313.

[12] P. Löb, R. Gleiter, unpublished results.

[13] R. Criegee, R. Askani, *Angew. Chem.* **1968**, *80*, 531−532; *Angew. Chem. Int. Ed. Engl.* **1968**, *7*, 537.

[14] I. R. Slagle, E. Ratajczak, D. Gutman, *J. Phys. Chem.* **1986**, *90*, 402−407.

[15] W. R. Roth, F. Hunold, M. Neumann, F. Bauer, *Liebigs Ann.* **1996**, 1679−1690.

[16] W. R. Roth, H.-W. Lennartz, W. v. E. Doering, L. Birladeanu, C. A. Guyton, T. Kitagawa, *J. Am. Chem. Soc.* **1990**, *112*, 1722−1732.

[17] W. v. E. Doering, W. R. Roth, *Tetrahedron* **1962**, *18*, 67−74.

[18] W. R. Roth, D. Wollweber, R. Offerhaus, V. Rekowski, H.-W. Lennartz, R. Sustmann, W. Müller, *Chem. Ber.* **1993**, *126*, 2701−2715.

[19] W. R. Roth, F. Hunold, *Liebigs Ann.* **1996**, 1917−1928.

[20] A. K. Cheng, F. A. L. Anet, J. Mioduski, J. Meinwald, *J. Am. Chem. Soc.* **1974**, *96*, 2887−2891.

[21] Dissertation, M. Boenke, Bochum **1994**.

[22] K. N. Houk, J. Gonzalez, Y. Li, *Acc. Chem. Res.* **1995**, *28*, 81−90; M. J. S. Dewar, C. Jie, *Acc. Chem. Res.* **1992**, *25*, 537−543.

[23] P. M. Kozlowski, M. Dupuis, E. R. Davidson, *J. Am. Chem. Soc.* **1995**, *117*, 774−778; H. Jiao, P. v. R. Schleyer, *Angew. Chem.* **1995**, *107*, 329−332; D. A. Hrovat, I. K. Morokuma, W. T. Borden, *J. Am. Chem. Soc.* **1994**, *116*, 1072−1076.

[24] B. O. Roos, *Adv. Chem. Phys.* **1987**, *69*, 339; B. O. Roos, *Int. J. Quantum Chem. Symp.* **1980**, *14*, 175.

[25] K. Anderson, P. A. Malmqvist, B. O. Roos, A. J. Sadlej, K. Wolkinski, *J. Phys. Chem.* **1990**, *94*, 5483−5488; K. Anderson, P. A. Malmqvist, B. O. Roos, *J. Chem. Phys.* **1992**, *96*, 1218−1226.

[26] When C_s-symmetry is assumed, **9** becomes a transition state connecting the two enantiomeric diradicals having C_1-symmetry. The resulting energy decrease is < 2 kcal·mol^{-1}.

[27] P. C. Hariaharan, J. A. Pople, *Theor. Chim. Acta*, **1973**, *28*, 213.

[28] M. Frisch, G. W. Trucks, H. B. Schlegel, P. M. W. Grill, B. G. Johnson, M. A. Robb, R. Cheeseman, T. Keith, G. A. Petersson, J. A. Montgomery, K. Raghavachari, M. A. Al-Jaham, V. G. Zakrzewski, J. V. Ortiz, J. B. Foresman, J. Cioslowski, B. Stefanov, A. Nanayakkara, M. Challacombe, C. Y. Peng, P. Y. Ayala, W. Chen, M. W. Wong, J. L. Andres, E. S. Replogie, R. Gomperts, R. L. Martin, D. J. Fox, J. S. Binkley, D. J. Defrees, J. Baker, J. P. Stewart, M. Head-Gordon, C. Gonzalez, J. A. Pople, Gaussian, Inc., Pittsburgh, **1995**.

[29] MOLCAS version 3, K. Andersson, M. R. A. Blomberg, M. P. Fülscher, V. Kellö, R. Lindh, P. A. Malmqvist, J. Noga, J. Olsen, B. O. Roos, A. J. Sadlej, P. E. M. Siegbahn, M. Urban, P.-O. Widmark, University of Lund, Sweden, **1994**.

[30] W. T. Borden, *Diradicals*, J. Wiley & Sons, New York, **1982**.

[31] W. Grimme, L. Schumachers, W. R. Roth, R. Breuckmann, *Chem. Ber.* **1981**, *114*, 3197−3208.

[97269]